In-situ fabrication of 3D interior hotspots templated with a protein@Au core–shell structure for label-free and on-site SERS detection of viral diseases

Iris Baffour Ansah[a,b,1], Soo Hyun Lee[a,1], Jun-Yeong Yang[a], ChaeWon Mun[a], Sunghoon Jung[a], Ho Sang Jung[a], Min-Young Lee[a], Taejoon Kang[c,d], Seunghun Lee[a], Dong-Ho Kim[a,b], and Sung-Gyu Park[a,*]

[a]*Nano-Bio Convergence Department, Korea Institute of Materials Science (KIMS), Changwon, Gyeongnam, 51508, Republic of Korea*

[b]*Advanced Materials Engineering Division, University of Science and Technology (UST), Daejeon, 34113, Republic of Korea*

[c]*Bionanotechnology Research Center, Korea Research Institute of Bioscience and Biotechnology (KRIBB), Daejeon, 34141, Republic of Korea*

[d]*School of Pharmacy, Sungkyunkwan University, Suwon, 16419, Republic of Korea*

[1]These authors contributed equally to this work.

[*]E-mail: sgpark@kims.re.kr

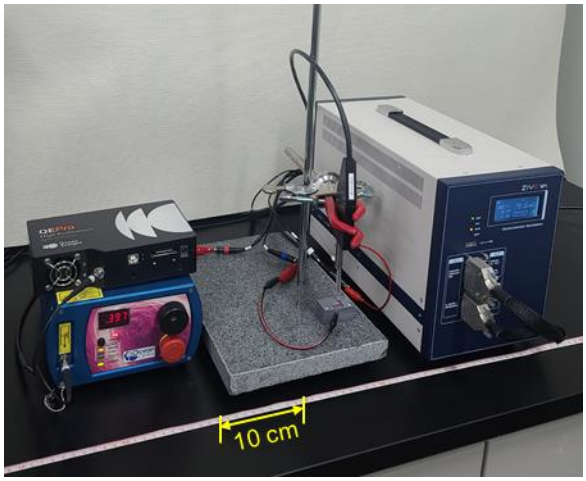

Fig. S1. Photographic image of the entire system used in this study.

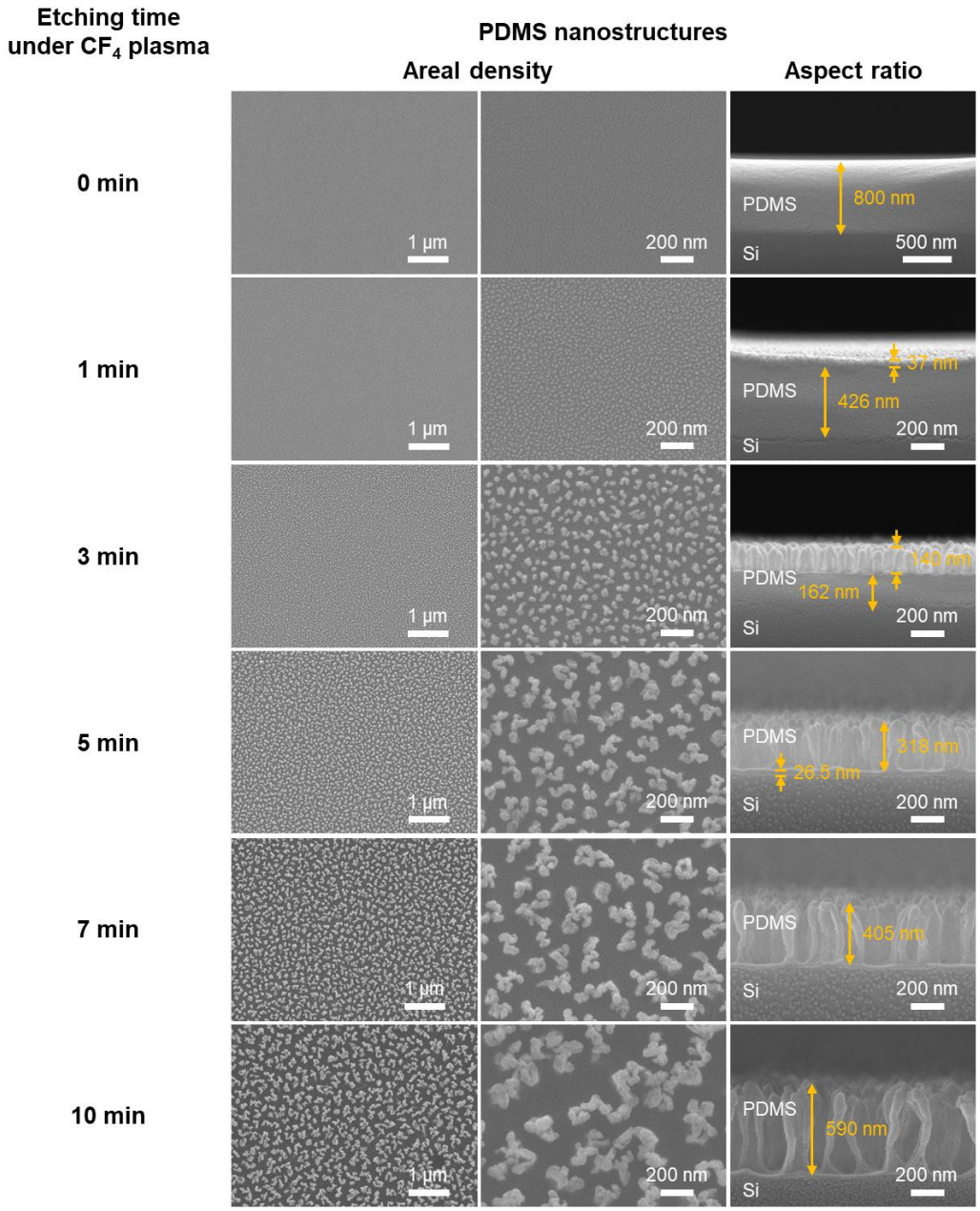

Fig. S2. Influence of CF_4 plasma etching time on morphological properties of the pristine MPs. Top-view and cross-sectional SEM images of the PDMS under CF_4 plasma etching for 0, 1, 3, 5, 7, and 10 min.

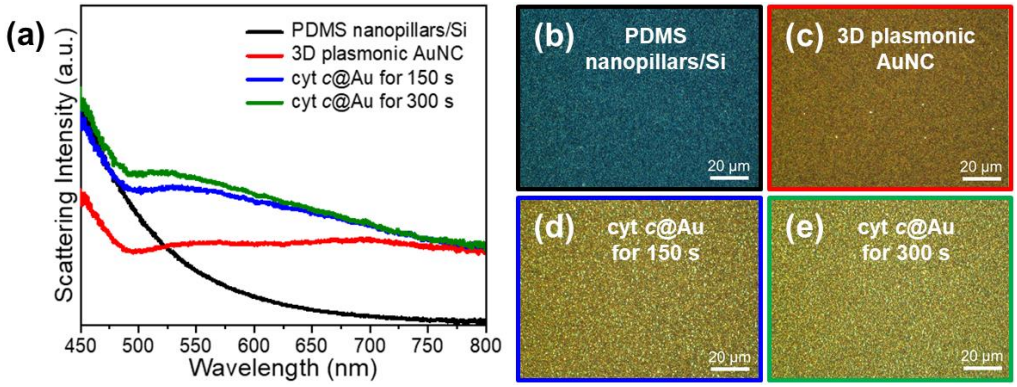

Fig. S3. Scattering characteristics of the substrates. (a) Dark scattering spectra of the PDMS nanopillars on the Si substrate (black), AuNC (red), and cyt *c*@Au for 150 s (blue) and 300 s (green) and (b–e) their true scattering color images.

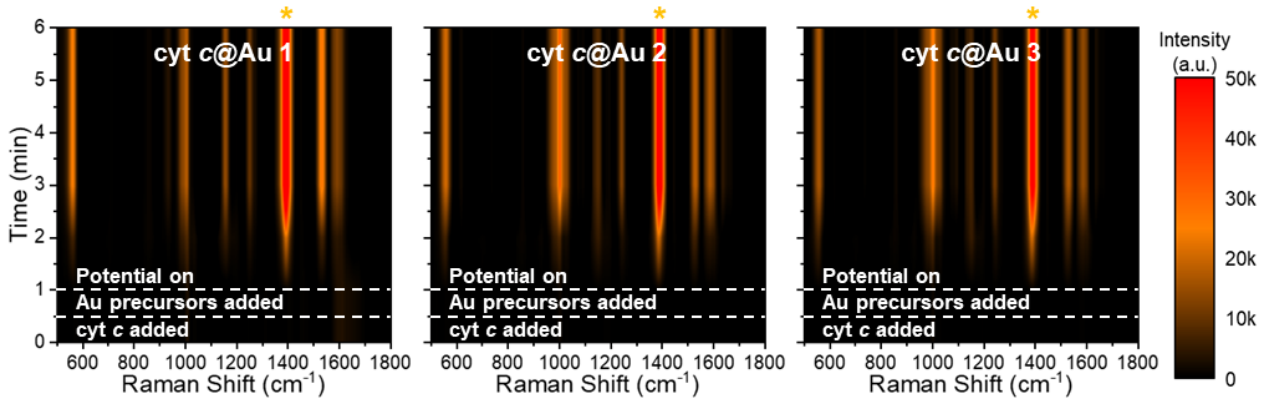

Fig. S4. Reproducibility of cyt *c*@Au core−shell samples. Temporal evolution of three different templates. The analytic peak of cyt c used in this study was marked with the asterisk (*).

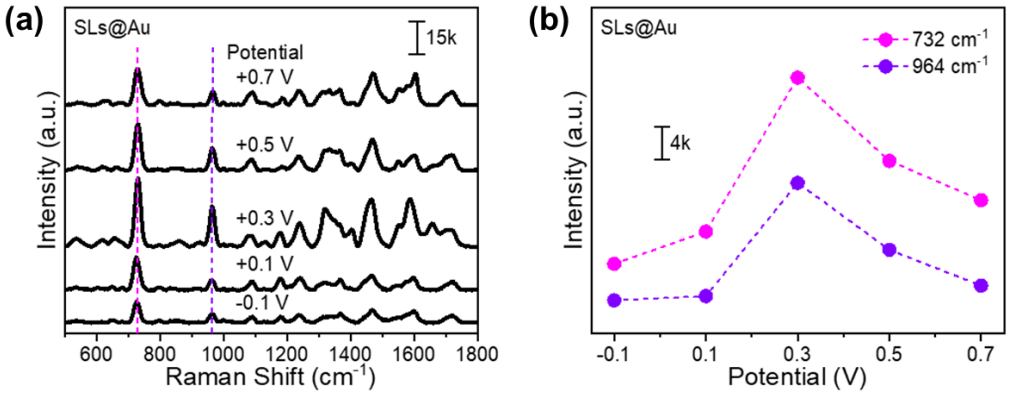

Fig. S5. Influence of applied potential on the SERS behaviors of the SLs@Au. (a) SERS spectra of the SLs@Au at different potentials and (b) the corresponding intensity profiles at the analytic peaks. The analytic peaks of SLs used in this study were marked with the dashed lines in (a).

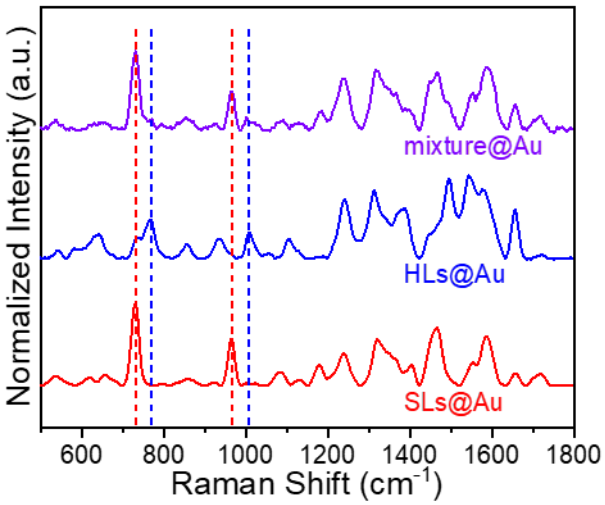

Fig. S6. Specificity and selectivity of the protein@Au templates. Normalized SERS spectra of the SLs@Au, HLs@Au, and their binary mixture@Au templates. The representative peaks of individual viral lysates were marked with dashed lines.

Raman shift (cm^{-1})	**Vibrational assignment**
551	Tryptophan
849	Tyrosine
925	C−C stretch
997	Phenylalanine
1022	Phenylalanine
1148	CN stretch
1185	Tyrosine
1237	Amide III
1380	Heme (v_4)
1441	CH_2 deformation
1518	Heme (v_3)
1575	Phenylalanine
1628	Heme (v_{10})

Table S1. Peak assignments of the cyt *c*.

Substrate	Labeling method	Dyes	LOD (PFU/mL)	Reference
Au nanopopcorns	aptamer DNA	Cy3 4-MBA	0.53	Chen et al., 2021
Hollow Au nanoparticles-assembled magnetic beads	reporter antibody detection antibody	MGITC	3.4	Cha et al., 2022
Hollow Au nanostars	capture antibody	MGITC	5.1	Yu et al., 2021
Microdroplet sensors	sandwich immunocomplex	SERS nanotag	0.22	Park et al., 2022
Protein@Au templates	-	-	2.2×10^{-2}	this work

Table S2. Comparison of strategical methodologies and LOD values for the detection of SLs based on the SLs@Au and other platforms.

Sample number	RT-PCR		LFA	protein@Au SERS templates		
	Ct value	P/N	P/N	Intensity (a.u.) at 732 cm^{-1}	Intensity (a.u.) at 964 cm^{-1}	P/N
1	16.80	P	P	7366.20	3053.94	P
2	20.32	P	P	5059.27	2186.19	P
3	22.90	P	P	3719.18	1782.53	P
4	30.25	P	N	2373.02	1066.99	P
5	33.85	P	N	1491.72	803.67	P
6	N.A.	N	N	237.95	324.87	N
7	N.A.	N	N	196.10	266.18	N
8	N.A.	N	N	367.29	468.35	N

Table S3. Comparison of RT-PCR, LFA, and protein@Au SERS templates for the diagnosis of clinical SLs (delta subtype).

References

Cha, H., Kim, H., Joung, Y., Kang, H., Moon, J., Jang, H., Park, S., Kwon, H.-J., Lee, I.-C., Kim, S., Yong, D., Yoon, S.-W., Park, S.-G., Guk, K., Lim, E.-K., Park, H.G., Choo, J., Jung, J., Kang, T., 2022. Surface-enhanced Raman scattering-based immunoassay for severe acute respiratory syndrome coronavirus 2, Biosens. Bioelectron. 202, 114008.

Chen, H., Park, S.-G., Choi, N., Kwon, H.-J., Kang, T., Lee, M.-K., Choo, J., 2021. Sensitive Detection of SARS-CoV-2 Using a SERS-Based Aptasensor. ACS Sens. 6, 2378−2385.

Park, S., Jeon, C.S., Choi, N., Moon, J.-I., Lee, K.M., Pyun, S.H., Kang, T., Choo, J., 2022. Sensitive and reproducible detection of SARS-CoV-2 using SERS-based microdroplet sensor, Chem. Eng. J. 446, 137085.

Yu, Q., Wu, Y., Kang, T., Choo, J., 2021. Development of surface-enhanced Raman scattering-based immunoassay platforms using hollow Au nanostars for reliable SARS-CoV-2 diagnosis, Bull. Korean Chem. Soc. 42, 1699−1705.